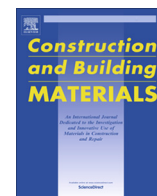Contents lists available at ScienceDirect

Construction and Building Materials

journal homepage: www.elsevier.com/locate/conbuildmat

Investigation on influential factors on chloride concentration index of cement-based materials by pore solution expression method

Xiang Hu [a,b,c], Caijun Shi [a,b,*], Deju Zhu [a,b], Geert de Schutter [c]

[a] Key Laboratory for Green & Advanced Civil Engineering Materials and Application Technology of Hunan Province, College of Civil Engineering, Hunan University, Changsha 410082, PR China
[b] International Science and Technology Innovation Centre for Green & Advanced Civil Engineering Materials of Hunan Province, College of Civil Engineering, Hunan University, Changsha 410082, PR China
[c] Magnel Laboratory for Concrete Research, Department of Structural Engineering, Ghent University, Ghent B-9052, Belgium

HIGHLIGHTS

- Effects of different factors on chloride concentration index (N_c) of cement paste are studied.
- Zeta potential, thickness and chloride distribution of EDL are investigated.
- The relationship between N_c and properties of EDL are modeled and studied.

ARTICLE INFO

ABSTRACT

In this study, the effects of different factors on chloride concentration index (N_c) of cement paste were studied. The factors including chloride concentration in soaking solution, slag replacement, external applied voltage and cation ions of soaking solution were all studied from the electrical double layer (EDL) properties point of view. Zeta potential and proton Nuclear Magnetic Resonance (^{1}H NMR) measurements were conducted to investigate the properties of electrical double layer for cement paste specimens and their effects on the value of chloride concentration index. The results showed that these factors all impacted effects on chloride concentration in electrical double layer and chloride concentration index. The properties of electrical double layer including chloride distribution and thickness of electrical double layer mainly controlled the phenomenon of "chloride concentrate" and value of chloride concentration index. As the increase of zeta potential and electrical double layer thickness, the content of chloride ions in electrical double layer and the value of chloride concentration index gradually increased.

1. Introduction

Chloride induced reinforcement corrosion has been one of the dominating problems leading to the deterioration of concrete structure. A significant amount of cost and efforts are paid every year all around the world for the maintenance, strengthening and even reconstruction on concrete structures threatened by chloride penetration and the induced reinforced corrosion. Within cement-based materials, the penetrated chloride ions can be captured by hydration products or components of raw materials, which is defined as chloride binding [1–3]. The free chloride ions in pore solution are major reason to cause the steel corrosion and studies

on extraction of pore solution and chloride concentration analysis have been extensively conducted [4].

Pore solution expression method with high pressure is considered as the most reliable method to acquire pore solution and study the free chloride concentration. Compared to other methods such as water extraction method (to obtain the water-soluble chloride), the results of pore solution expression are considered to be more close to the actual free chloride concentration. Duchesne and Bérubé [5] evaluated the validity of the pore solution expression method for determination of alkali concentrations in pore solution of hardened cement pastes and mortars. Their results showed that the alkali concentration in the expressed pore solution was not affected by the pressure at which the pastes and mortars were expressed, and the presence of aggregate did not bring any changes to the testing results. During the pore solution expres-

* Corresponding author.
   E-mail address: cshi@hnu.edu.cn (C. Shi).

sion, the pore structure of the testing sample was compressed and squeezed out the pore solution. During this process, the chloride ions in electrical double layer (EDL) can be extracted out together with the bulk pore solution by the high pressure. The chloride distribution and concentration in EDL are different from that in bulk pore solution due to the surface potential, which generally results into higher chloride concentration in the expressed pore solution in cement-based materials. This phenomenon was defined as "chloride concentrate" and chloride concentration index N_c was applied to define the ratio of chloride concentration in the expressed pore solution to that in soaking solution [6].

After discovering of chloride concentrate phenomenon in 1990s [6], extensive studies [7–9] have been conducted to investigate the mechanism of chloride concentrate and factors that may affect chloride concentration index. According to these studies, pore structure and EDL properties of cement-based are considered as predominate factors on value of N_c. In our previous studies, the variations of pore structure and chloride content during pore solution expression test were investigated and used to calculate the chloride concentration in the expressed pore solution. Moreover, the percentage of gel pores or small size pores in the total porosity is more important due to that the overlap of EDL in small size pores can significantly increase the chloride concentration in solution of EDL. For EDL properties, the Stern EDL model was generally applied to explain this phenomenon and present the chloride distribution in EDL. According to the EDL model established by Stern, the EDL consists of two layers [10]: internal layer and external layer. Internal layer refers to compact layer or Stern layer while external layer refers to the diffusive layer. In the compact layer, ions opposite to solid surface potential are strongly bound due to electrical or non-electrical attraction. Out of the compact layer, ions diffusively distribute in the diffusive layer, where the concentration of counter-ion (ion with opposite charge of ions in the compact layer) is higher than that of ions who take same charge as the compact layer (co-ions). With the increase of distance to solid surface, the concentration of counter-ion decreases until equal to that of bulk solution. In the diffusive layer, there exists a shear plane located close to the boundary layer between the compact and diffusive layers. The solution on the side of pore solution is flowable and able to moves with bulk pore solution. This movement generates a potential difference at the shear plane, which is defined as zeta potential [11,12]. The properties of EDL including zeta potential and thickness of EDL are also controllable for chloride concentration in EDL and in the expressed pore solution. He et al [8] calculated the chloride ion concentration in the expressed pore solution based on a proposed EDL model. However, the experimental results to confirm these models and calculations are insufficient. Therefore, a systematical analysis on influential factors from the EDL property point of view on chloride concentrate phenomenon and chloride concentration index is needed.

In this study, the factors influencing the chloride concentration in the expressed pore solution of cement paste specimens are investigated based on their effects on EDL properties of cement-based materials. Factors including chloride concentration in soaking solution, slag replacement, external applied voltage and cation ions of soaking solution are considered in this study. Zeta potential and proton nuclear magnetic resonance (^{1}H NMR) measurements are conducted to investigate the properties of EDL in different cement paste specimens and their effects on chloride concentration in the expressed pore solution and value of N_c. Based on the results presented in this study, the formation of the phenomenon "chloride concentrate" and its relationship with EDL or interfacial properties of cement-based material are illuminated. The results in this study can also lay a foundation on wider application of pore solution expression method in determining free chloride concentration in pore solution of cement-based materials.

2. Experimental

2.1. Raw materials

P·I 52.5 ordinary Portland cement (OPC) and Grade 95 slag powder (SL) were used in this study. The OPC has a specific surface area of 336 m^2/kg. The mortar compression strength is 26.6 and 57.3 MPa at 3 and 28 days, respectively, based on GB/T 17671-1999 (1999) (water/cement ratio = 0.5, sand/cement ratio = 3). The density and Blaine specific surface area of slag are 2900 kg/m^3 and 446 m^2/kg. The chemical composition of the cement and slag are given in Table 1, no chlorides are detected for materials used in this study. NaCl, KCl, CaCl$_2$ and AgNO$_3$ are analytical grade chemicals. Deionized water is used to prepare solution for chemical analysis.

2.2. Specimen preparation and curing

Cement pastes with water to binder (w/b) ratio 0.4 and different slag replacement levels (0, 20%, 40% and 60%) were prepared in this study. PVC pipes with a size of Φ50 × 200 mm were used as moulds. One end of the mold was sealed with polyvinyl chloride board. After cement paste was cast into the mold, the other end of the mold was sealed with plastic film immediately. After that, the specimens with mould were left in a room at 20 ± 2 °C for 24 h, then demolded and cut into thin-disc about 6 mm of thickness with a water-jet cutting machine.

The cement paste disc specimens were cured in water for 7 and 28 days, within which the last day of curing was 24 h of vacuum saturation with saturated limewater. Then pastes were immersed into 0.1, 0.3, 0.5, 0.7 and 1.0 mol/L of NaCl solutions respectively in plastic containers covered with plastic film at 20 °C. The volume ratio of soaking solution to specimens was kept above 40 times. The solution was replaced every two weeks to ensure the relatively constant chloride ion concentration in the soaking solution. The cement paste disc specimens were then soaked in NaCl solutions before pore solution expression and chloride ion analyses. For studies on types of cations, NaCl, KCl and CaCl$_2$ solutions were used as soaking solutions.

For studies with externally applied voltage, the specimens were prepared with Φ100 × 200 mm PVC pipe molds and cut into 8 mm thickness. After 28 days of bath curing, the cement paste specimens were separated into 2 groups. For the first group, the specimens were kept in water for another 207 days, followed by 60 h of rapid chloride migration (RCM) test according to Tang [13]. The catholyte solution was NaCl solutions with chloride concentration 0.1, 0.5 and 1.0 mol/L, 0.3 mol/L NaOH solution was used as anolyte solution. The applied voltage was 10 V. The pore solution expression and zeta potential measurement were conducted after 207 days of bath curing and 60 h of RCM test (210 days in total). As a reference group, cement paste specimens for natural diffusion were soaked in NaCl solution for 210 days after 28 days of bath curing.

2.3. Pore solution expression and chloride analysis

After the soaking process or RCM test, the specimens were rubbed with a cloth to obtain saturated surface dry condition. The specimens were crushed, placed into an expression apparatus and loaded to 510 MPa (900 kN) at a rate of 1.5–2.5 MPa/s. They were held at this pressure for 1 min, then unloaded rapidly and repeated once more. The expressed pore solution was collected with an injection syringe whose pinhead covered with a latex tubing to prevent leaking [14]. The collected pore solution was injected into a plastic container and sealed immediately to avoid carbonation. The pore solution expression apparatus was cleaned with unhydrous ethanol between two pore solution expressions to avoid cross contamination. For every batch, three specimens were used for pore solution expression, and the reported results are the average of the three specimens.

The collected pore solution was diluted 20 times for chloride ion titration with an automatic potentiometric titrator. The titration solution was 0.01 mol/L of AgCl solution. At the end point of the titration, automatic potentiometric titrator calculated the chloride concentration automatically according to potential-volume curve. "Chloride concentration index" N_c was calculated by the following equation:

$$N_c = c_k/c_b \tag{1}$$

where c_k is the chloride ion concentration determined by chloride ion titration, c_b is chloride ion concentration in exposure solution.

2.4. Zeta potential measurement

When the designed soaking time or RCM test period was reached, the samples were ground by ball mill and placed in a 60 °C vacuum drying oven for 24 h. The fraction of particles with diameter between 0.025 and 0.045 mm was collected by sieving for zeta potential measurement. The suspension was prepared by mixing powder samples and chloride solution with concentration equal to that of corresponding soaking solution. The mass ratio of solid to liquid was 1:1. The suspensions were kept on a stirring apparatus for 6 h, and kept still for one minute before the measurement. The zeta potential of the suspensions was measured with DT300 instrument.

Table 1
Chemical composition of raw materials (%).

Raw Material	SiO$_2$	Al$_2$O$_3$	Fe$_2$O$_3$	CaO	MgO	K$_2$O	SO$_3$	C	Ignition loss
OPC	22.51	5.32	3.78	63.13	2.56	0.71	2.02	–	–
SL	33.00	13.91	0.82	39.11	10.04	1.91	0.16	–	0.08

2.5. ^{1}H NMR test

^{1}H NMR relaxation tests were conducted for samples before pore solution expression test at room temperature (20.00 ± 5.00 °C) and low temperature ranged from 5 to −30 °C at a step of 5 °C. For low temperature point, the sample was kept in refrigerator with the testing temperature for 24 h before shifting to the NMR testing tube. Small fragments with around 0.5 cm diameter were used for NMR test. MicroMR12-025 produced by Niumag Corporation (Shanghai, China) was used for NMR relaxometry measurement. The resonance frequency was 11.845 MHz. Carr-Purcell-Meiboom-Gill (CPMG) pulse sequence was employed to measure NMR transverse relaxation time and the NMR results were transferred into pore size distribution according to the following equation proposed in Refs. [15–17]:

$$\frac{1}{T_2} \approx \frac{1}{T_{2,surf}} = \rho_2 \left(\frac{S}{V}\right)_{pore} = F_s \times \frac{\rho_2}{r} \qquad (2)$$

where T_2 is the transversal relaxation time of water; $T_{2,surf}$ is transversal relaxation time due to surface relaxation; $(S/V)_{pore}$ is specific surface area of pore; F_s is geometrical factor, $F_s = 2.0$ for cylinder pore; ρ_2 is surface relaxivity, here assumed 50 μm/s for cement mortars. Normally, the surface relaxivity rests with the "thickness" of surface layer, and average value of ρ was adopted in literatures [15,16]. In this study, it was assumed that the average surface relaxivity of the testing samples were identical, and an approximate value was decided to just qualitatively study the differences of pore size distribution between different samples.

2.6. Thermal analysis

A simultaneous thermal analyzer was used to conduct the thermal gravity analyses on hardened cement paste. Specimens were crushed by a hammer and moved through 2 mm sieve. These particles were immersed in unhydrous ethanol for at least 24 h to prohibit further hydration of cementitious materials. The particles were thoroughly ground with mortar and pestle after being cooled down. Powders smaller than 0.08 mm were placed in a vacuum oven at 105 °C for another 24 h of drying, and 10–15 mg of powders were used as testing samples. They were heated from 20 to 980 °C at heating rate of 10 °C/min in a nitrogen atmosphere. Recorded thermal gravity curves were used to determine the Friedel's salt and calcium hydroxide contents. For Friedel's salt, 6 water molecules will be decomposed at around 100–150 °C while another 6 molecules will be decomposed at around 300 °C according to Grishchenko et al. [18]. The content of Friedel's salt and Ca(OH)$_2$ can be calculated according to the mass loss at 300 and 450 °C, respectively.

2.7. Pore structure measurement

Pore structure measurements were carried out on specimens in parallel to pore solution expression. The specimens were crushed into fragments of about 0.5 cm in size. Their rough edges were chipped off by a plier. The small fragments were immersed in unhydrous ethanol for at least 24 h to stop further hydration, then dried in an oven at 60 °C until constant mass was reached. Pore structures of the dried cement pastes were measured by means of mercury intrusion porosimetry. Quantachrome PoreMaster 60 mercury injection apparatus shown in Figs. 3 and 4 was used in this study. The contact angle was assumed as 140°, and surface tension 106.7 psi/μm.

3. Results and discussions

3.1. Chloride concentration in soaking solution

Fig. 1 shows N_c of cement paste with 100% OPC after 7 and 28 days of curing and 91 days of soaking in NaCl solution. With the increase of chloride concentration, the value N_c gradually decreased.

The thickness of diffusive layer (L) can be calculated by Debye formula [9]:

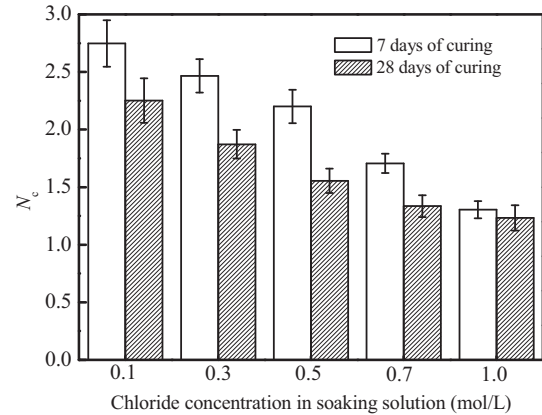$$L = k^{-1} = \sqrt{\frac{RT\varepsilon}{2F^2 c_b}} \qquad (3)$$

Fig. 1. Effects of chloride concentration in soaking solution on N_c of cement paste specimens with 100% OPC.

where, k is Debye constant, c_b is the concentration of bulk solution, ε is the dielectric constant, R is gas constant, T is room temperature, F is Faraday constant.

It can be seen from Eq. (3) that the effect of soaking solution concentration on thickness of diffusive layer in EDL is significant. The lower the concentration of NaCl solution is, the bigger the thickness of diffusive layer of cement pastes is. With the increase of EDL thickness, the solution and chloride ions in the diffusive layer can be increased, which can be extracted into the expressed pore solution during pore solution expression. Due to the decrease of EDL thickness, the chloride concentration in the expressed pore solution and value of N_c of paste specimens by pore solution expression gradually decreased. When immersed in chloride solution with higher concentration, the decreased EDL thickness weakened the effects of EDL on the expressed pore solution, thus the chloride concentration in the expressed pore solution might be close to that in the soaking solution and the value of N_c gradually decreased.

In order to investigate the relationship between chloride concentration in soaking solution and the thickness of EDL, the range of EDL was determined by low temperature ^{1}H NMR measurement in this study. As the temperature goes down to below zero, the pore solution in pores can be frozen to ice. Generally, the temperature for pore solution turns into solid phase relates to the size of pores where the pore solution stays. The smaller the pore size is, the lower the frozen temperature will be for the pore solution. Bager et al. [19,20] studied the ice formation in hardened cement pastes with low temperature Calvet microcalorimeter. They found that water contained in finer pores, physically adsorbed water in EDL formed on solid surface or in a "interlayer" position was non-frozen even under the condition of −55 °C, and the freezable (free) water within saturated cement paste specimens can be removed at a relative vapour pressure lower than 60% of atmospheric pressure. In order to increase the testing accuracy, the cement paste specimens after 7 days of curing were applied for ^{1}H NMR measurement to increase the porosity and water content within the specimens.

Fig. 2 shows the evolution of T_2 relaxation distribution within cement paste specimens with the decrease of temperature from 5 to −30 °C, experimental results of cement paste specimens
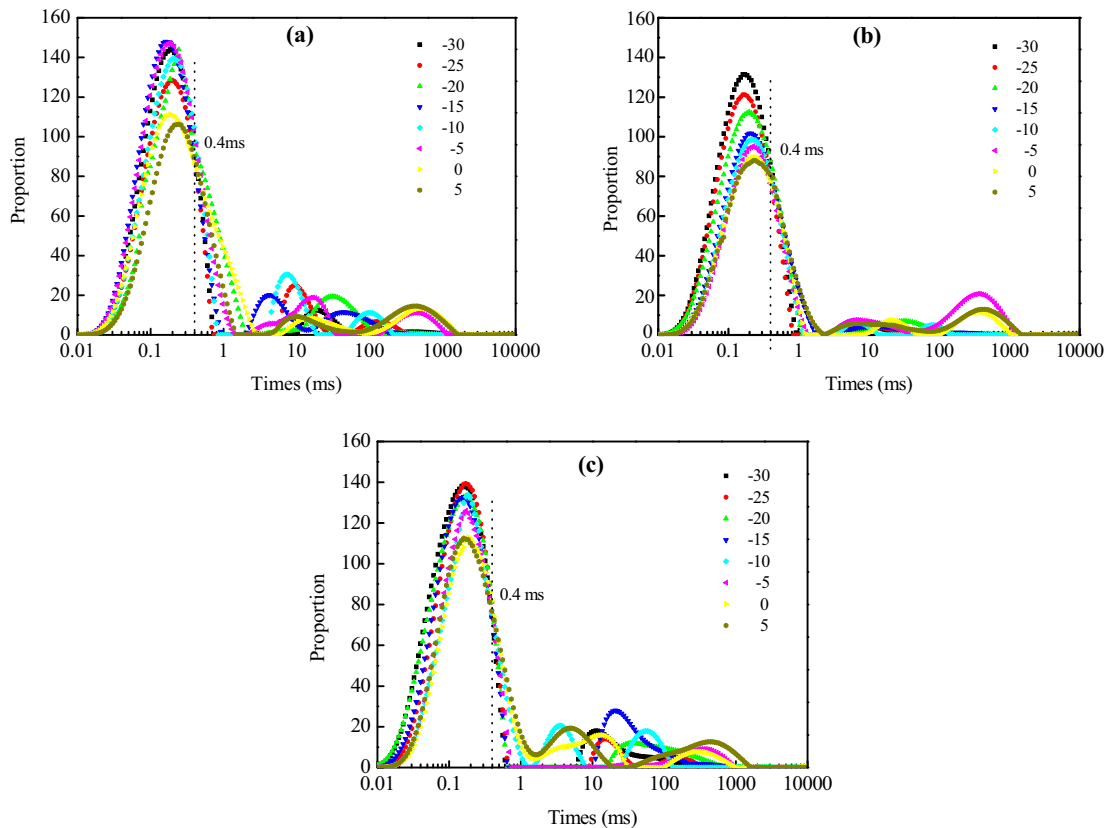
Fig. 2. T_2 relaxation distribution of cement paste specimens during freezing process after immersed in (a) 0.1 mol/L, (b) 0.5 mol/l and (c) 1.0 mol/L NaCl solution.

immersed in 0.1, 0.5 and 1.0 mol/L NaCl solutions are presented. It can be seen from the figures that the proportion of signal amplitude at right side, which relates to water in larger pores, gradually decreased while the left side increased. At the range of 100–10000 ms, T_2 signal was only detected under temperature of −5, 0 and 5 °C. Compared to the peak at the range of 0.01–1.0 ms, the T_2 signal on the right hand side of the T_2 relaxation distribution plot is relatively small, especially for cement paste specimens under lower temperature. When temperature decreased to −30 °C, nearly 95% of signals were located at the range of 0.01–1 ms. For the T_2 signal peaks with T_2 relaxation time in this section, it can be seen that the signal amplitude with relaxation time lower than 0.4 ms was increased with the decrease of temperature, while the signal decreased when relaxation time larger than 0.4 ms.

The value of T_2 in NMR measurement results can represent the location of water within samples. Large T_2 value relates to water in large pores, while the water in small pores and the adsorbed water in EDL can result into low T_2 value. In this study, we can easily regard the peak within 0.01 to 1.0 ms as the water in small pores and adsorbed water. Generally, the liquid in a pore has a frozen temperature related to the diameter of pore. Jehng et al. [21] studied the microstructural evolution of cement paste specimens by NMR, it was found that the capillary pore water can be frozen at temperature lower than −30 °C. However, water remained as liquid in gel pores over a temperature range reaching to −120 °C. The confinement of solid phase or solid surface on ions and liquid, which may change the existence form of solution within pore structure, was considered as the differences in freezing temperature.

It can be seen in this study that the water at the range of 0.01–1 ms remained to be liquid, the results in this section can be regarded as the water distribution before freezing. The effects of

surface potential on liquids and ions in EDL result into different properties of adsorbed water in EDL and free water in bulk pore. Due to the surface potential of solid phase, solution in EDL can be only partially moved parallel to solid phase, but not at the direction perpendicular to surface. In this study, the total content of water at the range of 0.01–1 ms was unchanged and we assumed that the water will not be transferred between small and large pores during the low temperature ^{1}H NMR measurement. It has been investigated [22] that the content of adsorbed water can be changed with different temperature. In this study, variation of adsorbed and free water should be opposite under the assumption that the total water content at the T_2 relaxation time from 0.01 to 1 ms unchanged. Therefore, it can be seen from the experimental results that the content of adsorbed water increases while free water decreases with the decrease of temperature. According to the T_2 relaxation distribution plots of cement paste specimens in different concentrations of NaCl solution shown in Fig. 2, it can be seen that the boundary points of T_2 relaxation time for adsorbed and free water of these three samples are basically same. On the two sides of 0.4 ms, the T_2 relaxation distribution plots show different trends with the decrease of temperature, which means the signal on these two sides presents two different types of pore water. Therefore, we determined T_2 = 0.4 ms as the boundary point for adsorbed and free water.

After the boundary point in T_2 distribution plots for adsorbed and free water is determined, the percentage of adsorbed water within cement paste specimens under ambient temperature (20 °C) can be calculated. The peak area of T_2 distribution represents the content of water, then the area between the plot and x axis on the left hand side of 0.4 ms was determined and divided by the total area of the distribution plot. Fig. 3 shows the percentage of adsorbed water to total water within cement paste speci-
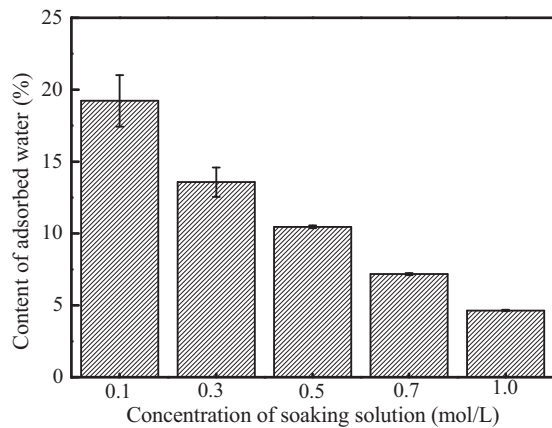
Fig. 3. Content of adsorbed water in cement paste specimens.

mens as a function of chloride concentration in soaking solution. It can be seen from the figure that the percentage of adsorbed water in cement paste specimens gradually decreases with the increase of concentration in pore solution or soaking solution. For cement paste specimens immersed in 0.1 mol/L NaCl solution, almost 20% of total water was adsorbed onto the surface of solid phase due to the larger EDL thickness, while it decreased to 5% as concentration increased to 1.0 mol/L.

According to the Stern EDL model, the distribution of chloride ions in EDL is different from that in bulk pore solution. With positive surface potential or zeta potential, the chloride ions diffusively distributed in EDL under the simultaneous effects of attraction from solid phase and thermal motion of ions. The value of N_c mainly controlled by two factors: the range of EDL and the chloride distribution or the average chloride concentration in EDL. It can be seen from Fig. 3 that the increase of chloride concentration in soaking solution decreases the range of EDL and also the adsorbed water content in EDL. He [8,23] calculated the thickness of EDL based on Stern model, it was found that the thickness of EDL decreased significantly with concentration of bulk solution, which became less obvious as the concentration higher than 0.5 mol/L. These findings can be used to interpret the decreased the value of N_c with the increase of chloride concentration in soaking solution.

The distribution of chloride ions and average chloride concentration in EDL are mainly affected by the surface potential or zeta potential. With higher surface potential, the amount of chloride ions being attracted into the EDL layer can be increased. Fig. 4
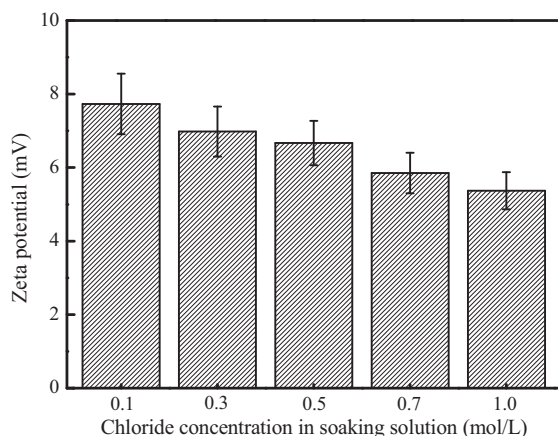

Fig. 4. Zeta potential of cement paste specimens after 7 days of bath curing and 91 days of soaking.

shows the zeta potential of hardened cement paste with 100% OPC after 7d of bath curing and 91d of soaking in different concentrations of NaCl solution. It can be seen that the zeta potential of cement paste specimens was decreased with the increase chloride concentration in soaking solution. According to Stern EDL model, the potential-determined layer, where ions are chemically bound onto the surface of solid occupies the most area of the compact layer. The ions in this layer, such as Ca^{2+} in the cement-based materials, also called as potential-determined ions. These ions are desolvated and generally determine the sign of zeta potential. Close to the potential-determined layer, there exists a thin layer with thickness equals to 1 or 2 molecules. The ions in this layer are solvated ions and are tightly adsorbed due to physical and electrostatic interactions [24]. In this layer, the concentration of ions with opposite charge to the potential-determined ions (named as counter-ions, Cl^- in this study) is higher and results into the decrease of potential. The potential increased from zero to maximum point in the potential-determined layer and went little bit lower to the boundary of compact and diffusive layers. Outside of the compact layer is the diffusive layer, in which most of the ions are flowable. With the increase of chloride concentration in pore solution, the concentration of counter-ions in the motionless layer between potential determined layer and diffusive layer increases and the potential decrease will be enhanced. The increase of chloride concentration can enlarge the difference between surface potential and zeta potential, which results into the decrease of zeta potential. In diffusive layer, the chloride concentration relates to the potential and gradually decreases with the increase of distance from solid surface. The chloride distribution and total chloride content within diffusive layer can be increased with the increase of zeta potential.

In conclusion, the increase of chloride concentration in soaking solution decreases the thickness of EDL and also the zeta potential, which results into the decrease of total chloride content in EDL. Therefore, with the increase of chloride concentration in soaking solution, the chloride concentration in the expressed pore solution and value of N_c gradually decreased.

3.2. Slag replacement

The chloride concentration indices N_c of cement paste specimens with different contents of slag are plotted in Fig. 5 as a function of soaking solution concentration. The results of cement paste specimens after 28 days of bath curing and different soaking ages including 56, 91 and 365 days are presented. It can be seen that after 56 days of soaking, the value of N_c decreased with the increase of slag replacement level. As the soaking time increased, the value of N_c all increased, especially for cement paste blended with slag. After 91 days of soaking, the value of N_c for 20% slag-blended cement paste specimens was slightly higher than that of OPC specimens. After soaking in NaCl solution for 1 year, it can be seen that almost all slag-blended cement paste specimens showed higher N_c values than that of OPC specimens. For all of the results shown in Fig. 5, the values of N_c were decreased with the increase of chloride concentration in soaking solution, which was in agreement with results and discussions in previous section.

Slag is a kind of binder with potential cementitious properties, the content of silica in slag is 33%, which is higher than that in OPC (21.09%). When slag is used to replace OPC, the quantity of C-S-H gel in hardened cement pastes may be increased due to pozzolanic reactions between slag and hydration products of OPC. Compared to 100% OPC specimens, hardened cement paste with slag can produce more [≡SiO—]. It will provide more adsorption groups. Therefore, the increase of C-S-H gel due to the slag replacement may enhance the ability of chloride adsorption which at last increases the concentration of chloride ion in the diffusive layer.
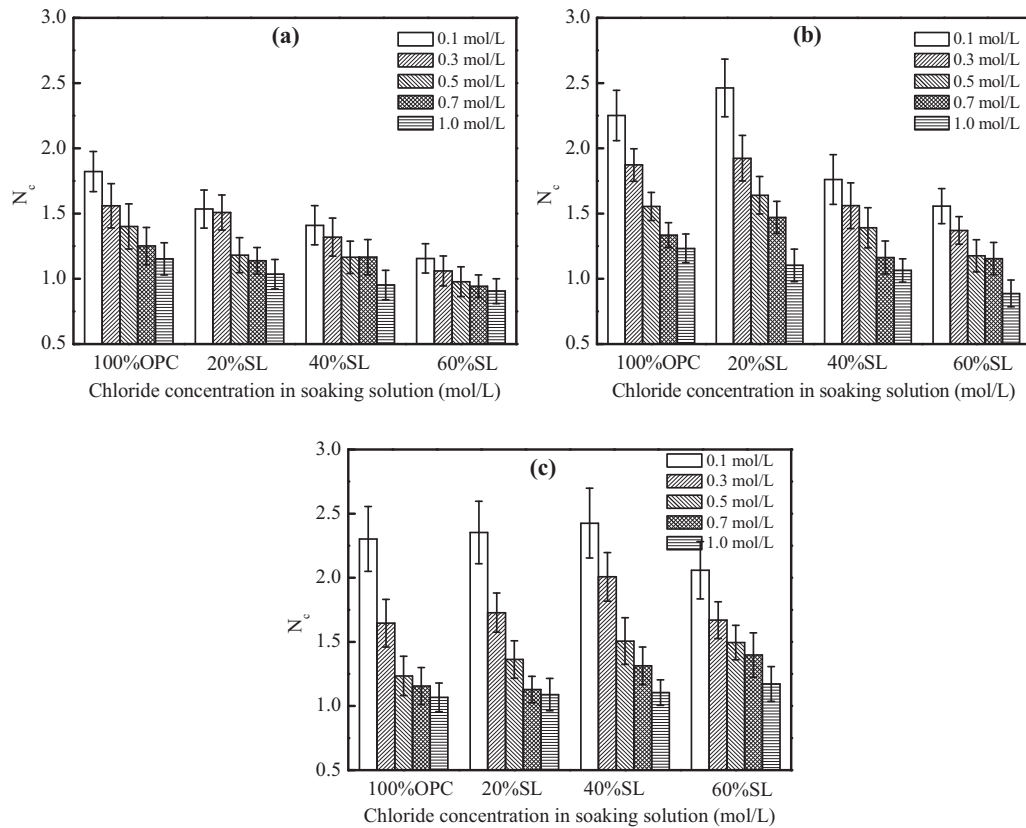
Fig. 5. Effect of slag content on N_c of cement paste specimens with 28 days of bath curing and (a) 56 days, (b) 91 days and (c) 365 days of soaking.

However, the reaction of slag falls behind the hydration of OPC and results into the lower content of C-S-H gel formed within cement paste at the early age [25]. Therefore, after 56d of soaking in NaCl solution, the addition of slag decreased the value of N_c. With the increase of soaking time, the reaction between slag and $Ca(OH)_2$ enhanced the formation of C-S-H in slag-blended paste and more adsorption sites for chloride ions were provided. It can be seen from Table 2 that with the increase of slag replacement level, the content of $Ca(OH)_2$ in cement paste specimens was gradually decreased. Fig. 6 shows the zeta potential of cement paste specimens with different slag replacement levels for similar curing and soaking ages as shown in Fig. 5. It can be seen that the zeta potential of the cement paste specimens decreased with the increase of slag content at the early age. However, with the increase of soaking time, the development of zeta potential in slag-blended cement paste specimens was faster than that of OPC specimens. After 1 year of soaking, the zeta potential of 100% OPC paste was similar or even smaller than that of the slag-blended specimens, which was in agreement with the value of N_c.

The increase of slag replacement led to a reduction of cement content, and decreased the content of primary hydration product $Ca(OH)_2$ significantly as shown in Table 2. These may have negative effects on pozzolan effects and the formation of C-S-H gel [25]. The decrease of cement and consumption of $Ca(OH)_2$ during pozzolanic reactions lower the pH of pore solution, even below 12.0 [26,27], which may show negative influences on dissociation of silanol group and chloride adsorption by C-S-H gel. Within cement-based materials, chloride can also be chemically bound by aluminum phases to form Friedel's salt [28]. The content of Friedel's salt within cement-based materials was increased with the increase of slag content as shown in Table 2. The content of Al_2O_3 in slag was higher than that in the cement while the content of sulfate was lower, which may enhance the chemical binding of cement pastes and formation of Friedel's salt. Chemical binding and physical adsorption in cement pastes coexist in a competitive dynamic process [29]. The enhancement of chemical binding would decrease the chloride concentration in pore solution and inhibit the physical adsorption of chloride ions onto EDL. This may also decrease the value N_c after slag replacement, especially at early soaking time with lower chloride concentration in pore solution. As the soaking time increased, the addition of slag enhanced the formation of C-S-H gel, which can provide more silanol site on the surface of hydration products and finally exceed the value of zeta potential for slag-blended samples compared to 100% OPC paste. The continually penetration of chloride ions from soaking solution can decrease the effects of chemical binding on chloride concentration in bulk pore solution. Therefore, the chloride content in EDL and value of N_c can be increased with the increased of slag replacement level.

Table 2
Thermal analysis results of cement paste specimens after 28 days of curing and 91 days of soaking.

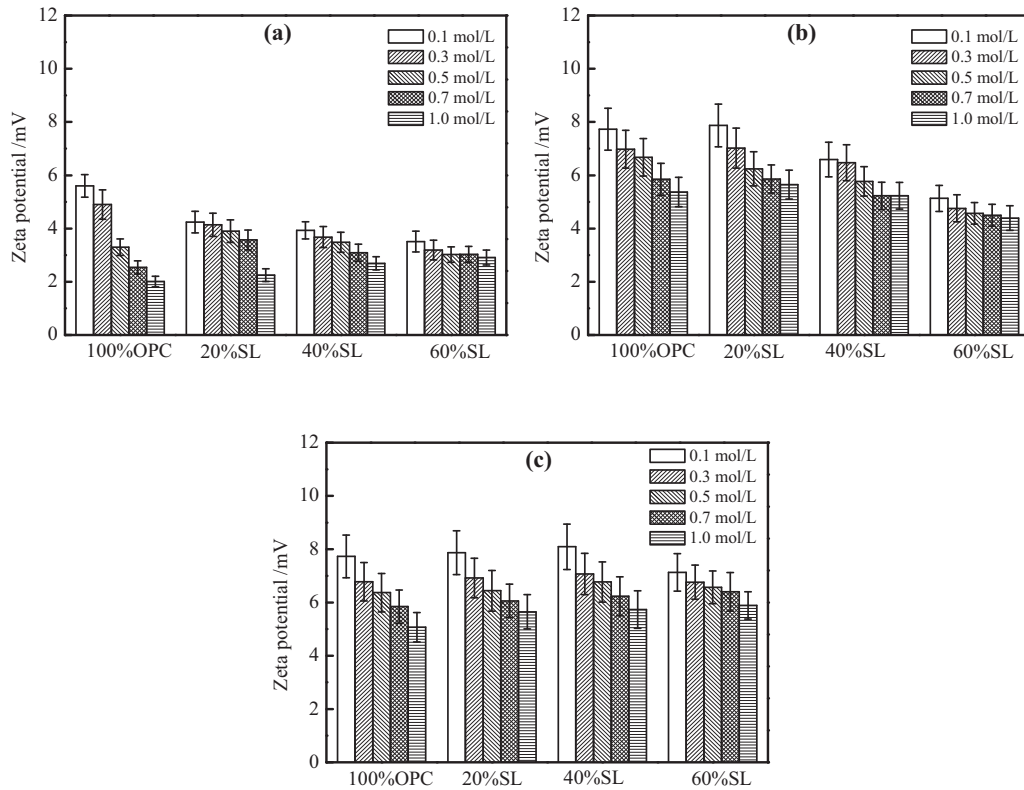| No.	Chloride concentration (mol/L)	$Ca(OH)_2$ (% of binder)	$Ca(OH)_2$ (% of OPC)	Friedel's salt (% of binder)
100%OPC	0.5	16.22	16.22	3.94
20%SL	0.5	9.07	11.34	4.81
40%SL	0.5	6.03	10.06	5.11
60%SL	0.5	2.87	7.17	5.97

Fig. 6. Zeta potential of cement paste specimens with 28 days of bath curing and (a) 56 days, (b) 91 days and (c) 365 days of soaking.

3.3. External applied voltage

Fig. 7 shows the value of N_c of cement paste specimens for natural diffusion (210 days of soaking) and RCM (60 h, followed by 207 days of bath curing) tests. The results showed that the value of N_c for cement paste specimens with applied voltage was much higher than that of natural immersion. The value of N_c constantly decreased with the increase of concentration of NaCl solution, while the declining rate for cement paste specimens with RCM test was greater. For cement paste specimens with RCM test, the value of N_c decreased from 3.6 to 1.8 when the chloride concentration in catholyte solution increased from 0.1 to 1.0 mol/L. As can be seen, the chloride concentration in soaking solution did not change the chloride content of OPC samples under natural immersion when the molarity of the solution increased from 0.5 to 1.0 mol/L.
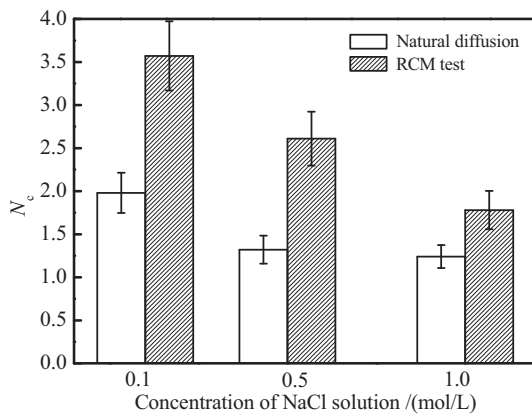
The applied voltage altered the microstructure and composition of hydration products, which are two major factors affecting the value of N_c of cement-based materials. For microstructure, the applied voltage accelerated the chloride migration and formation for Friedel's salt within cement paste, which decreased the porosity and higher the percentage of small pores. As shown in Table 3, the porosity of cement paste after RCM test was slightly decreased compared to that natural diffusion specimens. The mode pore size RCM test specimens was smaller while the percentage of small pores with diameter smaller than 50 nm was larger than the natural diffusion test specimens. For pores with smaller size, the effects of EDL on chloride concentration in the expressed pore solution can be enhanced as the chloride content in EDL unchanged. The applied voltage also altered the density and distribution of surface potential in hydration products and affected the zeta potential of EDL. Fig. 8 shows the zeta potential of hardened cement paste after soaking in NaCl solution and RCM test, the result of bath cured sample is also presented as reference. For bath curing samples, the OH^- ions in pore solution can be attracted by the surface potential and diffusively distributed in diffusive layer. The zeta potential of reference sample was about 3.9 mV. For chloride exposed samples, the value of zeta potential was decreased with the increase of sodium chloride concentration in the solution both for diffusion and rapid migration tests. The zeta potentials of samples subjected to RCM test were higher than that of samples with natural immersion, especially for samples exposed to lower sodium chloride concentration solutions. As discussed above, the chloride concentration in EDL was increased with larger zeta potential. In this study, higher N_c was obtained in cement paste specimens with external applied voltage due to larger zeta potential caused by the applied voltage.

Results showed that the differences of N_c between natural diffusion and RCM test decreased as the chloride concentration in soaking and catholyte solutions increased. The diffusion of chloride

Fig. 7. N_c of cement paste specimens with 100% OPC.

Table 3
Pore size distribution of cement paste samples with 100% OPC.

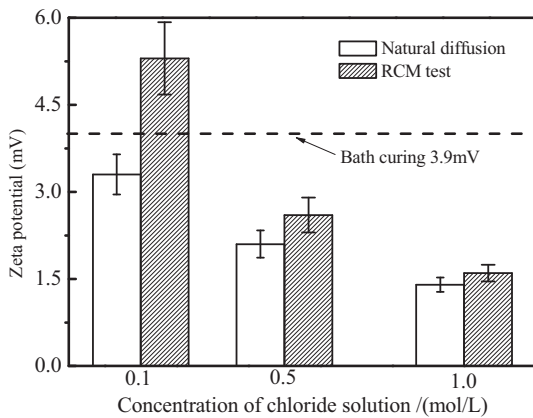| Conditions	Density/g.cc^{-1}	Total porosity/%	Mode size/nm	Pore size distribution/nm			
				5–10	10–50	50–1000	>1000
Natural soaking	2.12	18.16	18.51	17.90	63.23	14.10	4.77
Electro migration	2.14	18.02	17.35	20.71	63.57	9.22	6.50

Fig. 8. Zeta potential of hardened cement paste with 100% OPC.

from external solution to interior pore solution was initiated and determined by the concentration gradient. However, the applied electric field can accelerate the penetration of chloride ions. When the concentration of external solution was lower, the concentration gradient force was weak and the chloride migration in pore solution was more controlled by the applied voltage. With the increase of chloride concentration in the soaking solution, the concentration gradient force gradually enhanced and increased the chloride concentration in EDL and bulk pore solution. Therefore, the gap between concentration indexes for samples in two groups were gradually narrowed as the concentration in soaking solution increased, which can be also seen from the effects of applied voltage on zeta potential shown in Fig. 8.

3.4. Cation ions

Fig. 9 shows the value of N_c of cement paste specimens after 28 days of curing and 91 days of soaking in different cation types of chloride 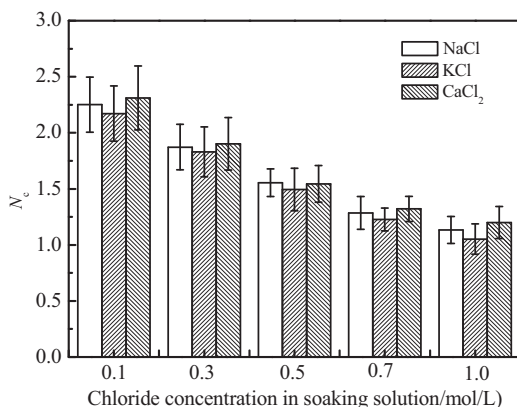solution. It can be seen from the figure that for cement paste specimens immersed in NaCl, KCl and CaCl$_2$ solutions, CaCl$_2$ immersed samples obtained the highest chloride concentration in the expressed pore solution, followed by NaCl and KCl solution. For all of these specimens, the value of N_c decreased with the increase of chloride concentration in soaking solution.

According to the description and discussion on EDL model presented above, the type and concentration of co-ions and counterions are important for zeta potential and ion distribution within EDL. In previous studies [30], the chloride binding capacity of cement pastes on sodium chloride and calcium chloride were detected and compared. It was found that more chloride ions can be adsorbed by hydration products for CaCl$_2$ solution immersed samples. For zeta potential of cement pastes, calcium ions are more important and mostly the sign and value of zeta potential are controlled by the concentration of calcium ions in pore solution [31]. Viallis-Terrisse et al. [32] reported that the value of zeta potential of C-S-H gel was gradually increased with increase of calcium ion concentration in solution and calcium ions were considered as the potential-determining cation ion for the C-S-H surface. Fig. 10 is the zeta potential of cement paste specimens with different chloride solution after 28 days of curing and 91 days of soaking. It can be seen that the zeta potential of samples immersed in CaCl$_2$ solution was much higher than that of other two chloride solutions, while no obvious differences were obtained for NaCl and KCl solutions. The variations of zeta potential with chloride concentration and cation ions in soaking solution are similar to that of N_c shown in Fig. 9. With the increase of zeta potential, more chloride ions can be absorbed and increase the chloride concentration in EDL. Fig. 11 is the total chloride content of samples after 28 days of curing and 91 days of soaking in chloride solution with different cations and concentrations. It can be found that for samples immersed in calcium chloride solution, more chloride ions can be adsorbed compared to sodium chloride and potassium chloride solutions. Generally, a similar role is played by sodium and potassium ions for chloride adsorption within EDL and on the surface of hydration products. In this study, the chloride binding capacity of
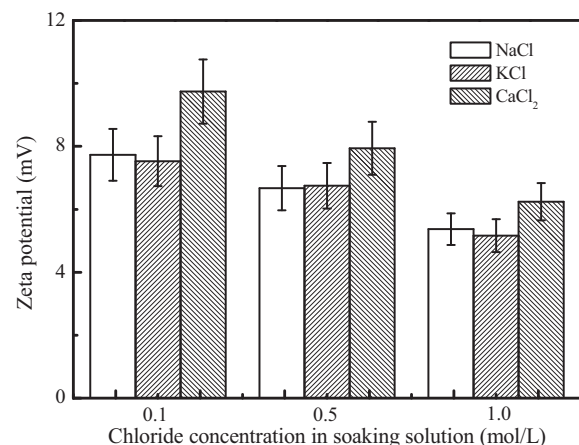

Fig. 9. N_c of cement paste specimens after 91 days of soaking in chloride solution with different cations.

Fig. 10. Zeta potential of cement paste specimens with different types of chloride solution.
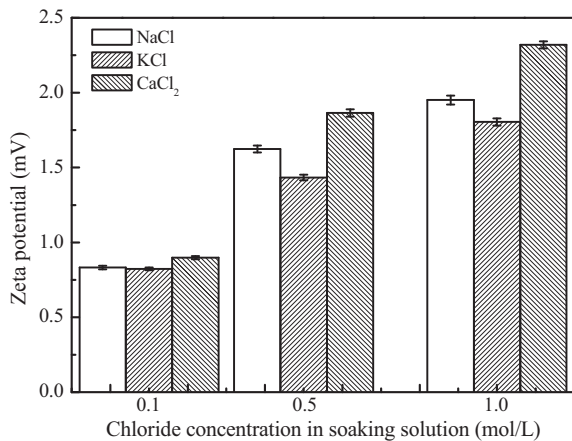
Fig. 11. Total chloride content of cement paste specimens with different types of chloride solution.

sodium chloride was slightly higher than that of potassium chloride.

4. Conclusions

In this study, the influential factors on chloride concentration index of cement paste specimens by pore solution expression method are studied, zeta potential and other properties of EDL formed at the solid–liquid interface are considered. With the aid of results and discussions, the mechanism of chloride concentrate phenomenon and chloride concentration index can be illuminated. Besides, this study can also lay a foundation for the application of pore solution expression method in determining the free chloride concentration of cement-based materials. According to the results and discussions presented above, the following conclusions can be drawn:

1. With the increase of chloride concentration in pore solution, the thickness of EDL layer gradually decreased, which decreased the percentage of adsorbed water content. The value of zeta potential also decreased with chloride concentration, which resulted into the decrease of chloride concentration in the expressed pore solution and value of N_c.
2. The slag-blended cement paste specimens showed low zeta potential and N_c than cement paste without slag at early age due to the lower early hydration rate. However, the addition slag enhanced the formation of C-S-H gel as the soaking age increased, which increased the zeta potential and value of N_c for cement paste specimens after 1 year of soaking in chloride solution.
3. The external applied voltage changed the distribution of surface potential and increased the zeta potential, the chloride concentration in the expressed pore solution of cement paste specimens was increased after RCM test.
4. When $CaCl_2$ solution was applied as soaking solution, the content of chloride ions adsorbed in EDL was increased due to the increase of zeta potential. The values of N_c for NaCl and KCl immersed samples were similar and both lower than that of $CaCl_2$ immersed cement paste specimens.

Declaration of Competing Interest

The authors declare that they have no known competing financial interests or personal relationships that could have appeared to influence the work reported in this paper.

References

[1] J.O. Ukpata, P. Basheer, L. Black, Slag hydration and chloride binding in slag cements exposed to a combined chloride-sulphate solution, Constr. Build. Mater. 195 (2019) 238–248.
[2] M. Khan, O. Kayali, Chloride binding ability and the onset corrosion threat on alkali-activated GGBFS and binary blend pastes, Eur. J. Environ. Civ. Eng. 22 (2018) 1023–1039.
[3] M. Gbozee, K. Zheng, F. He, X. Zeng, The influence of aluminum from metakaolin on chemical binding of chloride ions in hydrated cement pastes, Appl. Clay Sci. 158 (2018) 186–194.
[4] Q. Yuan, C. Shi, G. De Schutter, K. Audenaert, D. Deng, Chloride binding of cement-based materials subjected to external chloride environment–a review, Constr. Build. Mater. 23 (2009) 1–13.
[5] J. Duchesne, M. Bérubé, Evaluation of the validity of the pore solution expression method from hardened cement pastes and mortars, Cem. Concr. Res. 24 (1994) 456–462.
[6] S. Nagataki, N. Otsuki, T.-H. Wee, K. Nakashita, Condensation of chloride ion in hardened cement matrix materials and on embedded steel bars, Mater. J. 90 (1993) 323–332.
[7] Q. Li, C. Shi, F. He, S. Xu, X. Hu, X. Wang, Y. Chang, Factors influencing free chloride ion condensation in cement-based materials, J. Chin. Ceramic Soc. 41 (2013) 320–327.
[8] F. He, C. Shi, X. Hu, R. Wang, Z. Shi, Q. Li, P. Li, X. An, Calculation of chloride ion concentration in expressed pore solution of cement-based materials exposed to a chloride salt solution, Cem. Concr. Res. 89 (2016) 168–176.
[9] H. Friedmann, O. Amiri, A. Aït-Mokhtar, Physical modeling of the electrical double layer effects on multispecies ions transport in cement-based materials, Cem. Concr. Res. 38 (2008) 1394–1400.
[10] D. Lowke, C. Gehlen, The zeta potential of cement and additions in cementitious suspensions with high solid fraction, Cem. Concr. Res. 95 (2017) 195–204.
[11] Y. Elakneswaran, T. Nawa, K. Kurumisawa, Electrokinetic potential of hydrated cement in relation to adsorption of chlorides, Cem. Concr. Res. 39 (2009) 340–344.
[12] Y. Elakneswaran, T. Nawa, K. Kurumisawa, Zeta potential study of paste blends with slag, Cem. Concr. Compos. 31 (2009) 72–76.
[13] L. Tang, Chloride Transport in Concrete-Measurement and Prediction, Chalmers University of Technology, 1996.
[14] R. Luo, Y. Cai, C. Wang, X. Huang, Study of chloride binding and diffusion in GGBS concrete, Cem. Concr. Res. 33 (2003) 1–7.
[15] H.Y. Carr, E.M. Purcell, Effects of diffusion on free precession in nuclear magnetic resonance experiments, Phys. Rev. 94 (1954) 630.
[16] A. Valori, P.J. McDonald, K.L. Scrivener, The morphology of C-S-H: lessons from H nuclear magnetic resonance relaxometry, Cem. Concr. Res. 49 (2013) 65–81.
[17] A. Valori, P.J. McDonald, K.L. Scrivener, The morphology of C-S-H: lessons from H nuclear magnetic resonance relaxometry, Cem. Concr. Res. 49 (2013) 65–81.
[18] R.O. Grishchenko, A.L. Emelina, P.Y. Makarov, Thermodynamic properties and thermal behavior of Friedel's salt, Thermochim. Acta 570 (2013) 74–79.
[19] D.H. Bager, E.J. Sellevold, Ice formation in hardened cement paste, part I—Room temperature cured pastes with variable moisture contents, Cem. Concr. Res. 16 (1986) 709–720.
[20] D.H. Bager, E.J. Sellevold, Ice formation in hardened cement paste, Part II—drying and resaturation on room temperature cured pastes, Cem. Concr. Res. 16 (1986) 835–844.
[21] J.-Y. Jehng, D. Sprague, W. Halperin, Pore structure of hydrating cement paste by magnetic resonance relaxation analysis and freezing, Magn. Reson. Imaging 14 (1996) 785–791.
[22] R. Yong, P. Taylor, B.P. Warkentin, Swelling pressures of sodium montmorillonite at depressed temperatures, Clays Clay Miner. 11 (1962) 268–281.
[23] F. He, Measurement of Chloride Migration in Cement-Based Materials using AgNO3 Colorimetric Method, Central South University, Changsha, 2010.
[24] K.A. Klein, J.C. Santamarina, Electrical conductivity in soils: underlying phenomena, J. Environ. Eng. Geophys. 8 (2003) 263–273.
[25] H. Yu, Z. Weng, W. Sun, H. Chen, J. Zhang, Influences of slag content on chlorine ion binding capacity of concrete, J. Chin. Ceramic Soc. 35 (2007) 801.
[26] U. Wiens, W. Breit, P. Schiessl, Influence of high silica fume and high fly ash contents on alkalinity of pore solution and protection of steel against corrosion, Special Publ. 153 (1995) 741–762.
[27] F. He, C. Shi, Q. Yuan, K. Zheng, Q. Zou, Factors influencing chloride concentration at the color change boundary using AgNO3 colorimetric method, J. Chin. Ceramic Soc. 36 (2008) 890–895.
[28] X. Wang, C. Shi, F. He, Q. Yuan, D. Wang, Y. Huang, Q. Li, Chloride binding and its effects on microstructure of cement-based materials, J. Chin. Ceram. Soc. 41 (2013) 187–198.
[29] R. Luo, Y. Cai, C. Wang, Binding capability of chloride ions in mortar and paste with ground granulated blast furnace slag, J. Build. Mater. 4 (2001) 148–153.

[30] E. Nägele, The zeta-potential of cement: Part II: effect of pH-value, Cem. Concr. Res. 16 (1986) 853–863.

[31] E. Nägele, The zeta-potential of cement: Part III: the non-equilibrium double layer on cement, Cem. Concr. Res. 17 (1987) 573–580.

[32] H. Viallis-Terrisse, A. Nonat, J.-C. Petit, Zeta-potential study of calcium silicate hydrates interacting with alkaline cations, J. Colloid Interface Sci. 244 (2001) 58–65.